

Fluxon Devices

Shigeki SAKAI, Hiroshi AKOH, Akihiko YAGI and Hisao HAYAKAWA

Electrotechnical Laboratory,

1-1-4 Umezono, Sakura-mura, Niihari-gun, Ibaraki 305, Japan

New fluxon devices, i.e., a fluxon feedback oscillator and a fluxon transfer device are proposed. The successful operations of both devices are obtained by using Josephson samplers. The fluxon feedback oscillator realizes a oscillation state consisting of a fluxon-pulse train. The oscillation period can be controlled between 35 and 70 ps. The essential memory-device operation of the fluxon transfer device is confirmed. Possible applications of the fluxon devices are also discussed.

There has been much interest in fluxons moving in a Josephson transmission line (JTL). Here, we propose and describe a group of new devices called 'fluxon devices'. We believe that the devices will become essential elements for constructing new application fields. One example of them is the fluxon feedback oscillator, and another is the fluxon transfer device. We have obtained successful operations of both devices using a Josephson sampling technique.

1. Fluxon Feedback Oscillator

The fluxon feedback oscillator (FFO) makes an oscillation state consisting of a pulse train. The width of a pulse determined by the feature of inherent fluxon motions is very narrow, and its typical value is less than 5 ps.¹⁾ The oscillation frequency depending on the length of the JTL can be controlled by dc bias currents fed to the JTL. The maximum oscillation frequency is roughly estimated to be the inverse of twice the half-width of a pulse. This means that the maximum oscillation frequency is 250~500 GHz if the width is 1~2 ps.

The structure of the FFO is shown in Fig 1. The junction is formed between a widely spreading lower superconductor and an upper superconductor curved like a ring, forming a ring-shaped JTL. Both edges of the upper superconductor are connected with a feedback resistor R_f . At one edge A of the JTL, the device has a terminal to which a dc current I_e and a trigger impulse current I_p can be applied. An output circuit, a load resistor R_L

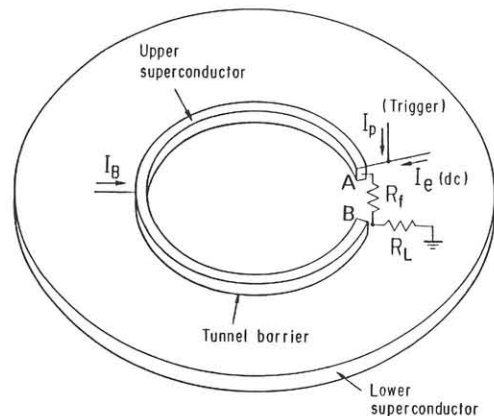


Fig. 1. Structure of the fluxon feedback oscillator.

in the case of Fig. 1, is connected to the other edge B.

The operational principle is as follows. Initially, the dc current I_e is supplied to the JTL under the condition of $I_e < I_e^0$, where I_e^0 is the threshold current to keep the JTL in the zero voltage state. Next, by applying a trigger impulse current I_p , a fluxon is generated at this side of the JTL. The generated fluxon moves toward the edge B. It disappears at this edge, and at the same time the vortex current of the fluxon is absorbed into R_f as well as R_L , because the values of R_f and R_L are chosen so that the load impedance (a function of R_f and R_L) connected to the edge B is the order of the characteristic impedance of the JTL.²⁾ Thus, the feedback current I_f flowing in R_f is added to I_e . Then, a fluxon is generated once again and moves to the edge B. The above process is repeated infinitely, i.e., an oscillation.

tion state is realized. The value of I_e affects the oscillation period, since the initial velocity of the generated fluxon increases with increasing I_e . The oscillation period can also be controlled by changing a dc current I_B fed to a middle point on the JTL as shown in Fig. 1, because the Lorentz force due to I_B changes the velocity of the fluxon.

Figure 2 shows a photograph of an actually fabricated sample. It consists of a ring-shaped JTL, a trigger pulse generator (TPG) and a Josephson sampler (JS). The JTL is made by the NbN/NbN junction where the barrier is formed by the niobium oxide.³⁾ It is $2.5 \mu\text{m}$ wide and $95 \mu\text{m}$ long. (The diameter of the ring is $\sim 34 \mu\text{m}$.) NbN has the large magnetic penetration depth λ_L . Since the larger λ_L results in the smaller Josephson penetration depth λ_J which gives a measure of the spatial spreading of a fluxon, NbN is attractive for making the device small. Resistors are made by Au-In films. The TPG and the JS are fabricated by the Pb-alloy technology. The TPG gives a single shot signal.⁴⁾ The JS is constructed by a direct coupled Josephson sampler.⁵⁾

Figure 3 shows the waveform obtained at $I_e/I_e^0 = 0.69$ and $I_B/I_B^0 = 0.20$, where I_e^0 is 0.48 mA and I_B^0 (the threshold current of I_B) is 0.98 mA . In this case, the oscillation period is 38.0 ps (The oscillation frequency is 26.3 GHz). The half-width of each pulse is $\sim 11 \text{ ps}$, which is ~ 4 times larger than that obtained from the computer simulation. The difference is thought to be due to the deterioration of the resolution of the Josephson sampling system caused by jitters and crosstalks. The critical current density I_0 of the JTL is 1.9 kA/cm^2 . Then, we obtain $\lambda_J = 5.0 \mu\text{m}$

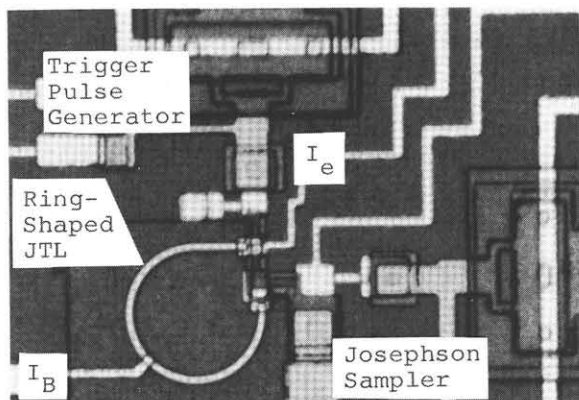


Fig. 2. Photograph of a fabricated FFO.

which satisfies the relation $I_e^0 = 2\lambda_J w I_0$,⁶⁾ where w is the width of the JTL. The length of the JTL becomes $19\lambda_J$. The upper NbN is $0.7 \mu\text{m}$ thick and the lower is $1.0 \mu\text{m}$ thick. The JTL has the normal resistance R_{NN} of $93 \Omega\mu\text{m}^2$ and the sub-gap resistance R_{SG} of $463 \Omega\mu\text{m}^2$. The sheet resistance of the Au-In film is 1.0Ω . The critical current density of the Pb-alloy junctions is 3.9 kA/cm^2 .

The dependence of the oscillation period T on I_e and I_B is shown in Fig. 4. As shown in Fig. 4, T is controlled between 35 and 70 ps by changing I_B and I_e . When I_e is less than 0.27 mA , the oscillation is not observed, whether I_B is applied or not. This means that the generation of a fluxon is not affected by the existence of I_B . This is easily understood by the fact that the spatial spreading of I_e ($\sim 2\lambda_J$) and I_B ($\sim 4\lambda_J$) are much smaller than the separation ($\sim 11\lambda_J$) between the feedpoint of I_B and that of I_e (i.e., the edge).

The solid lines in Fig. 4 represent the result of the computer simulation performed by using a circuit analysis program. The values of $L = 0.69 \text{ pH}/\square$ and $C = 12 \text{ pF}/\text{cm}^2$ are used in the simulation, where L and C is the sheet inductance and the capacitance per unit area of the JTL, respectively.⁷⁾

The energy carried by a fluxon is the order

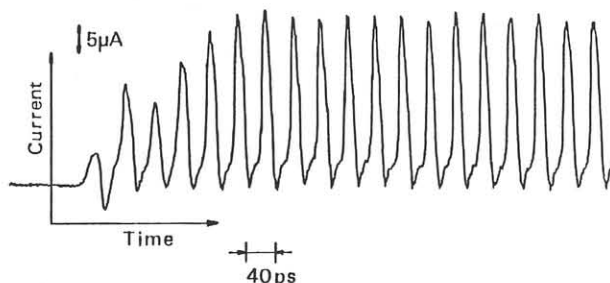


Fig. 3. An oscillation waveform at $I_e/I_e^0 = 0.69$ and $I_B/I_B^0 = 0.20$. The oscillation period is 38.0 ps .

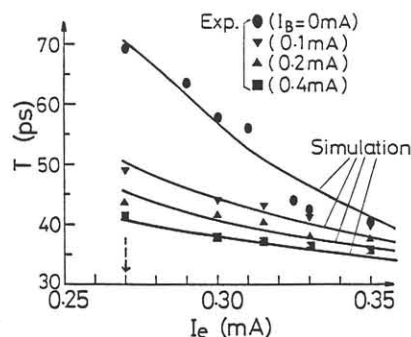


Fig. 4. Dependence of the oscillation period T on I_e and I_B . The solid lines are the simulation results.

of $10^{-17} \sim 10^{-19}$ J.⁸⁾ If the oscillation period is $10 \sim 100$ ps, then the power is estimated to be $10^{-6} \sim 10^{-9}$ W.

The FFO gives us important functions for various kinds of circuit applications. It can be operated as a memory device, in which an oscillation state corresponds to the storage of information "1", and non-oscillation state corresponds to "0". The size of the memory is decided by the loop size. According to the simulation, the oscillation states can be realized even in the case where the JTL length is $\sim 4\lambda_J$. If we choose $\lambda_L = 2800 \text{ \AA}$ (NbN)⁷⁾ and $I_0 = 3 \text{ kA/cm}^2$, then, we obtain $\lambda_J \sim 4 \text{ \mu m}$, resulting in the loop diameter of $\sim 5 \text{ \mu m}$ ($4\lambda_J/\pi$).

The FFO may also be used for high frequency signal sources such as local oscillators of the Josephson or SIS mixers and a signal source offering an ultra-high clock rate of the Josephson A-D converter.

2. Fluxon Transfer Device

The fluxon transfer device (FTD) consists of a JTL with partially resistive shunted regions as shown in Fig. 5. A fluxon can be intentionally stopped at the resistive shunted region, (i.e. information is stored,) and can be moved by applying a drive current to the region (i.e., information is transferred). This phenomenon is interpreted qualitatively as follows. A fluxon generated at one edge intends to move toward to the other edge. However, when it enters into the resistive shunted region, it loses the kinetic energy ($CV^2/2$) because the energy is absorbed into the shunted resistor. Then, the fluxon cannot go ahead and back if we choose the size of the resistor so that it stops at this region. According to the computer simulation, the range of the

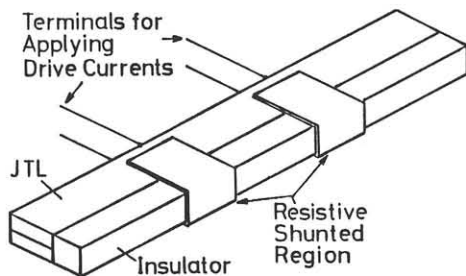


Fig. 5. Structure of the fluxon transfer device.

size of the resistor required for realizing this function is fairly wide. For example, if the length of the resistor is $\sim 2\lambda_J$, and $R_{SG}/R_{NN} \sim 5$, this function is realized by choosing $R_{SU}/(R_{NN}/w) \sim 0.3$, where R_{SU} is the resistance of the shunted resistor per unit length. When a drive current is applied to the region, the fluxon begins to move.

Figure 6(a) is a photograph of a fabricated sample, and Fig. 6(b) shows its schematic diagram. A NbN/NbN JTL with dimensions of $2.5 \text{ \mu m} \times 120 \text{ \mu m}$ has a resistive shunted region. The dimensions of the resistor made by a Au-In film is $8 \text{ \mu m} \times 6 \text{ \mu m}$. To this region, a terminal to which a dc current I_{DD} is supplied and a latch generating circuit (LG) are connected. To one edge of the JTL a pulse generating circuit (PG) and a terminal for supplying a dc edge current I_e are connected. To the other edge of the JTL a JS is connected. The output of the LG is connected to the Josephson sampling gate through a resistor in order to estimate the delay time of the fluxon signal from the latch signal applied by the LG. The PG, LG and JS are fabricated by the Pb-alloy technology.

Results of the Josephson sampling observation are shown in Fig. 7. Figure 7(a) shows the waveform obtained at $I_e/I_e^0 = 0.12$ on the condition that, before a fluxon is generated at one edge, the dc drive current I_{DD} is applied ($I_{DD}/I_{DD}^0 =$

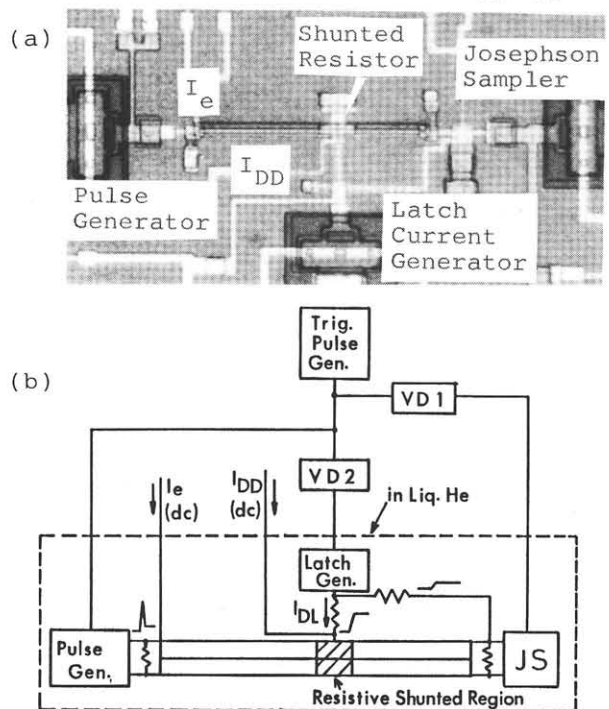


Fig. 6. (a) Photograph and (b) schematic diagram of a fabricated FTD.

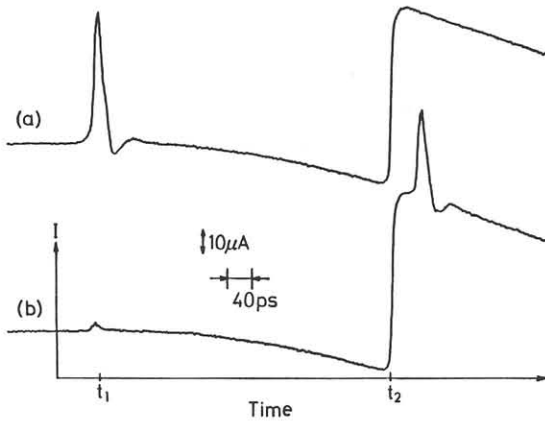


Fig. 7. Results of the Josephson sampling observation at $I_e/I_e^0 = 0.12$.
 (a) $I_{DD}/I_{DD}^0 = 0.15$. (b) $I_{DD} = 0$.

0.15). This sample has I_e^0 of 0.66 mA and I_{DD}^0 of 1.3 mA and I_0 of 3.5 kA/cm², where I_e^0 and I_{DD}^0 are the threshold currents of I_e and I_D , respectively. Then we obtain $\lambda_J = 3.8 \mu\text{m}$. The sheet resistance of the Au-In film is 1.0 Ω/\square . The first pulse found at $t=t_1$ in Fig. 7(a) is the signal of a fluxon which reaches the JS circuit without stopping at the resistive shunted region. In this case, since I_{DD} is applied in advance, a fluxon generated at one edge never stops at this region. The reference latch signal synchronizing with the current I_{DL} supplied from the LG is found $t=t_2$. Since there is no fluxon in the JTL when I_{DL} is applied, no fluxon pulse is superimposed to the reference latch signal.

Figure 7(b) is the waveform obtained under the same condition in the case of Fig. 7(a) except that I_{DD} is set to be zero. In this case, fluxon signals at $t=t_1$ are not found. On the other hand, a fluxon signal is found after the latch signal is applied ($t=t_2$). This means that a generated fluxon stops at the resistive shunted region, and begins to move by applying the latch signal. From Fig. 7 it can be said that the fluxon is hold in the resistive shunted region at least for $\sim 500\text{ps}$. The delay time at this read-out operation is $\sim 50\text{ps}$, which agrees fairly well with the computer simulation result.

Figure 8 shows a quasi-static operation of the sample to demonstrate a memory operation. At the clock 'a' an input signal I_w , which triggers a 3-junction interferometer in the PG to generate a fluxon in the JTL, is applied. No output signal appears at this clock. This means that a generated

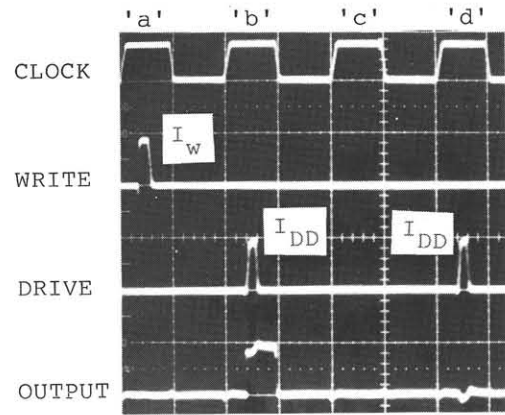


Fig. 8. Quasi-static operation of the fluxon transfer device. (X: 50 $\mu\text{s}/\text{div.}$)

fluxon is stored at the resistive shunted region. At the clock 'b' when a drive current I_{DD} is applied to this region, we can see an output latch signal at the Josephson sampling gate, which means the stored fluxon is read out. At the clock 'c' no input current is applied. Then, at the clock 'd' an output signal, of course, does not appear. These can be an essential memory device operation. Figure 8 also shows the stored information is hold in the resistive shunted region at least for the order of 100 μs .

The FTD will be used for memory devices and shift registers. The dimensions of the device depend on λ_J . If we choose $\lambda_L = 2800 \text{ \AA}$ (NbN) and $I_0 = 6\text{kA}/\text{cm}^2$, then, we obtain $\lambda_J \sim 2.8\mu\text{m}$, which makes the devices considerably small.

In summary, a fluxon feedback oscillator and a fluxon transfer device are proposed. The successful operations of both devices are obtained. The oscillation period of the fluxon feedback oscillator is controlled between 35 and 70 ps. The essential memory-device operation of the fluxon transfer device is confirmed.

References

- 1) S. Sakai, H. Akoh and H. Hayakawa: Jpn. J. Appl. Phys. 22 (1983) L479.
- 2) P.L. Christiansen and O.H. Olsen: Physica 1D (1980) 412.
- 3) A. Shoji, S. Kosaka, F. Shinoki, M. Aoyagi and H. Hayakawa: IEEE Trans. Magn. MAG-19 (1983) 827.
- 4) S.M. Faris: Appl. Phys. Lett. 36 (1980) 1005.
- 5) H. Akoh, S. Sakai, A. Yagi and H. Hayakawa: Jpn. J. Appl. Phys. 22 (1983) L435.
- 6) R. Vaglio: J. Low Temp. Phys. 25 (1976) 299.
- 7) A. Shoji and M. Aoyagi: private communication.
- 8) S. Sakai and H. Tateno: Jpn. J. Appl. Phys. 22 (1983) 1374.